

Adsorption Behavior of the Primary, Secondary and Tertiary Alkyl, Allyl and Aryl Alcohols Over Nanoscale (1 0 0) Surface of γ -Alumina

Mehdi Zamani^{1,2*}, Hossein A. Dabbagh^{2*}

1) Department of Chemistry, Malek-ashtar University of Technology, Shahin-shahr P.O. Box 83145/115, Islamic Republic of Iran

2) Department of Chemistry, Isfahan University of Technology, Isfahan 84156-83111, Islamic Republic of Iran

Abstract

In this study, the adsorption behavior of the primary, secondary and tertiary alcohols over nanoscale (1 0 0) surface of defect spinel γ -alumina was investigated with the aid of density functional theory (DFT) at BLYP/DNP level of calculation. The influence of different substituents including alkyl, cycloalkyl, allyl and aryl were analyzed for free and adsorbed alcohols to shed light the adsorption selectivity of these compounds over γ -alumina surface. These results indicate that more branches at α position of alcohol favor the adsorption, while a decrease in adsorption energy is achieved for the alcohols containing the substituents at the β position. The tertiary alcohols are adsorbed over the surface stronger than secondary and primary alcohols. Alcohols with larger alkyl chains have greater adsorption energies. Also the aryl alcohols are adsorbed over the surface better than the alkyl and allyl moieties.

Keywords: Nanoscale surface of γ -Alumina; Alcohol; Molecular adsorption; DFT

© 2014 Published by Journal of Nanoanalysis.

1. Introduction

Alumina is well known catalyst by both acidic and basic properties. In recent years, many experimental and theoretical works have studied the structure, reactivity and selectivity of γ -alumina especially at nanoscale (1-23). Theoretical investigations of the adsorption on γ -alumina have focused mostly on Lewis acidity of the surface (1-4), and the reactivity with water (5-11), hydrogen sulfide (5,10,12), carbon monoxide (5,10,13), ammonia (6), pyridine (4,6), hydrogen chloride (7), alkenes (14,15), alkanes (16), alcohols (17-23) and ethers (23).

* Corresponding authors. *E-mail address*: m.zamani@ch.iut.ac.ir; dabbagh@cc.iut.ac.ir

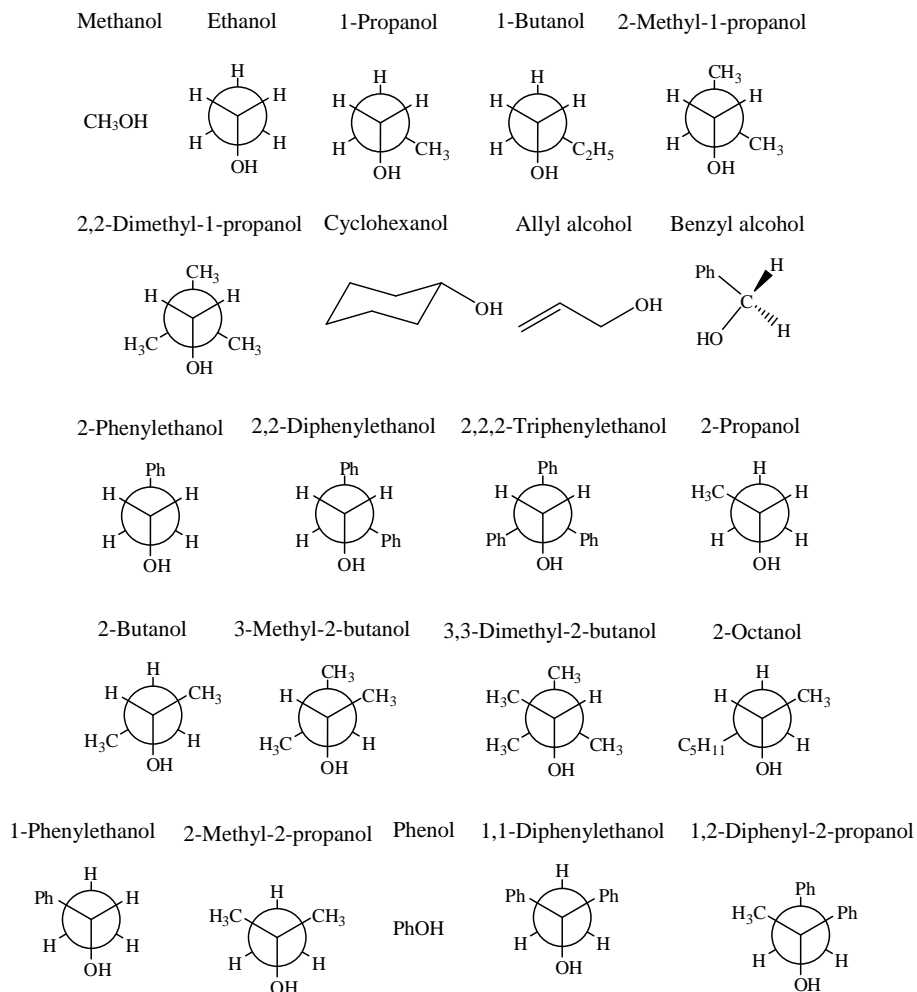


Fig. 1. Structure and Newman projection of the considered alcohols

The conceptions which describe the surface properties of different aluminas are quite interesting. Peri (24) first proposed a model of the surface of alumina based on the hypothesis that the planes exposed preferentially are those of index (1 0 0), thus explaining the observed adsorption bands of five types of surface hydroxyl groups in infrared spectra. Although this model does not sufficiently describe all of the surface properties, it is still of considerable interest. Knozinger and Ratnasamy (25) proposed a detailed model as an extension of the Peri model. Their basic assumption was that the mixtures of low-index crystal planes, i.e. (1 0 0), (1 1 0) and (1 1 1), are exposed on the surface of the crystallites. The relative abundance of different faces is assumed to vary for different aluminas. Five types of OH groups were considered, corresponding to the coordination of the hydroxyl groups, either to tetrahedral or to octahedral aluminum atoms, to a combination of each, or to both. Later Busca et al. (26) proposed another empirical model which takes into account cationic vacancies onto the surface coupled with OH assignment for well-known and characterized compounds.

The quantum chemical calculations have recently developed some new models of γ -alumina based on the cluster model (5,12,14,16,17,27-30) or periodic slab on the surface (4,10,12,31-37). Sohlberg et al. reported the presence of various amounts of hydrogen within the bulk structure of spinel γ -alumina (27). They proposed that γ -alumina is a sequence of hydrogen-containing compounds. But, Wolverton and Hass (38) indicated that hydrogen spinel is thermodynamically unstable with respect to decomposition into an

anhydrous defect spinel plus boehmite. Raybaud and co-workers reported a complete nonspinel structure based on molecular dynamic simulations and DFT calculations of the dehydration of boehmite (4,31-33,39). Nelson and coworkers performed DFT and simulated XRD calculations for identification of three different spinel-related γ -alumina structures (fully and partly hydrogenated structures and defect spinel) versus nonspinel models (40,41). They predicted that the spinel related structure model is better than the nonspinel model could describe the bulk structure of γ - Al_2O_3 . Also, Ferreira et al. reported that the spinel model is thermodynamically more stable and the infrared spectrum complement the experimental data (42).

γ -Alumina is used as catalyst for conversion of alcohols to alkenes (43), ketones (44) and ethers (45). Molecular adsorption of alcohols on the surface of γ -alumina occurs before the starting of these reactions. Theoretical investigations of the alcohols adsorption on γ -alumina have been limited to methanol (17,18), ethanol (18), 1-propanol (18), 2-propanol (18,21) and a number of recently publications of the present authors about 2-butanol (19), 2-octanol (20) and 1,2-diphenyl-2-propanol (20). In this study, we report the adsorption behavior of variety aliphatic and aromatic alcohols containing the alkyl, cycloalkyl, allyl and aryl substituents (Figure 1). Our purpose of this work is the estimating adsorption energy of various alcohols over γ -alumina nanoscale (100) surface. Certainly, the alcohols with greater adsorption energy can do better dehydration and dehydrogenation reactions; on the other words, the conversion of these alcohols over γ -alumina is high.

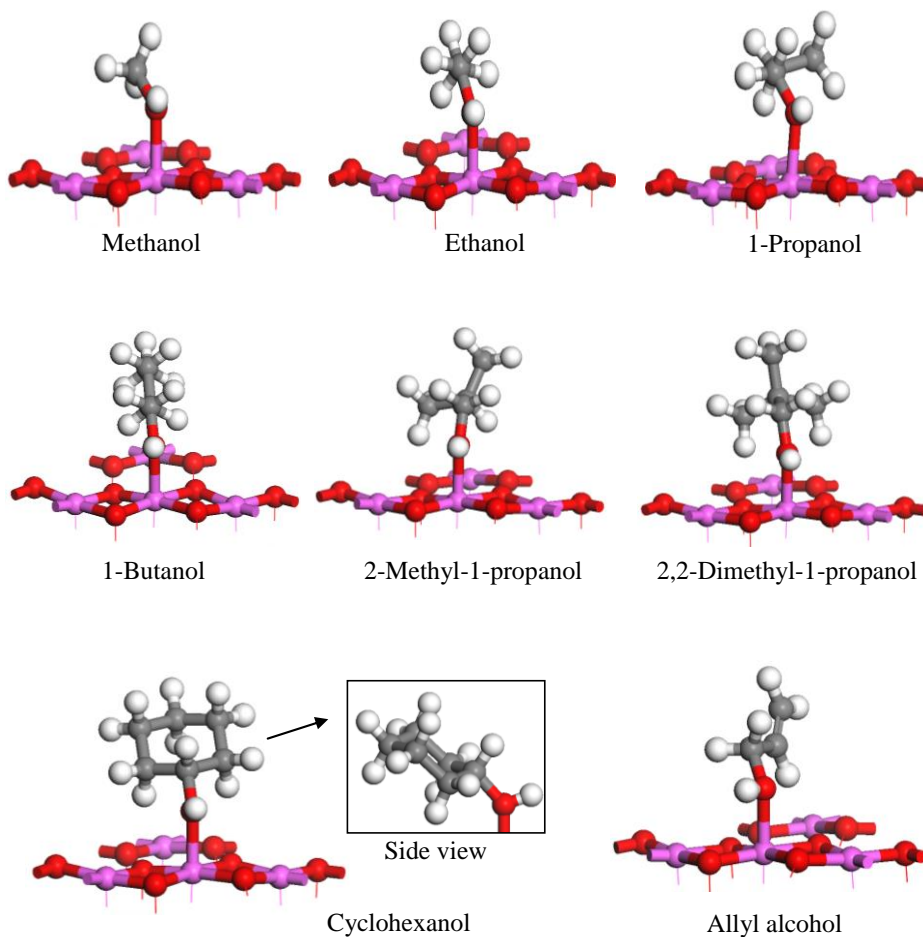


Fig. 2. The global minimum optimized geometry of considered alcohols after adsorption over nanoscale (1 0 0) surface of γ -alumina calculated at BLYP/DNP level of theory

2. Computational details

In this paper we focused our studies on the nanoscale (1 0 0) surface of γ -alumina defect spinel structure which has been proposed in our earlier studies (19,20). We imposed a vacuum of 15 Å between slabs in the direction of the crystal lattice, perpendicular to the surface plane, and periodically repeated the unit cell through space. To speed up our calculations, we selected two layers of atoms while the bottom layer of the slab was constrained. Both aluminum and oxygen atoms are present on these surfaces; aluminum atoms (violet color) are Lewis acid sites, whereas oxygen atoms (red color) are Brønsted basic sites. Our DFT calculations were performed using the DMOL3 code (46,47). The Double Numerical Plus Polarization function (DNP) and BLYP generalized gradient approximation were used in all calculations. Each basis function is restricted to a cutoff radius of 5 Å. Effective core potentials (ECP) were used to treat the core electrons and a k-point set separation of 0.07 Å⁻¹. The tolerance of the energy change was set for all calculations to 2.0e-5 Ha. For determining the adsorption selectivity of alcohols over penta-coordinated aluminum atoms in (1 0 0) surface, the adsorption energy (ΔE_{ads}) was calculated via equation (1); where $E_{\text{(adsorbed alcohol on surface)}}$ refers to the energy of the system after adsorption, and $E_{\text{(alcohols)}}$ and $E_{\text{(surface)}}$ refer to the energy of an isolated alcohol molecule and the bare surface. A negative energy corresponds to a stable molecule-surface system.

$$\Delta E_{\text{ads}} = E_{\text{(adsorbed alcohol on surface)}} - E_{\text{(alcohol)}} - E_{\text{(surface)}} \quad (1)$$

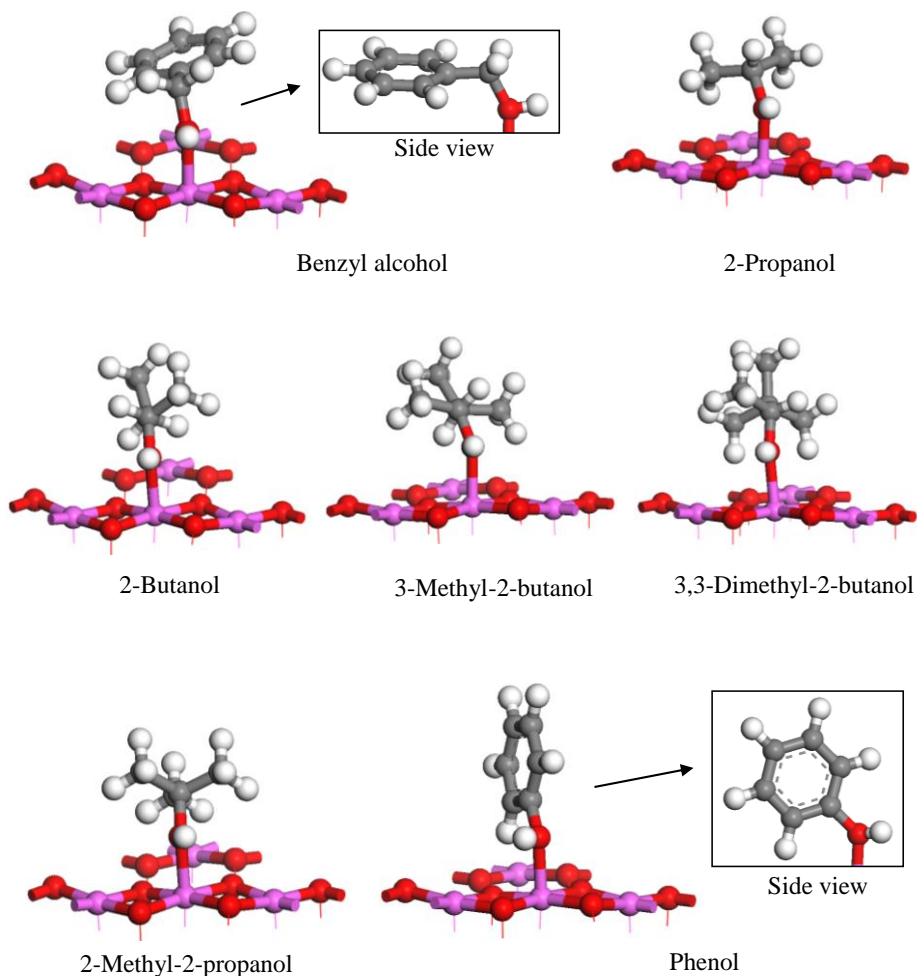


Fig. 2. Continued

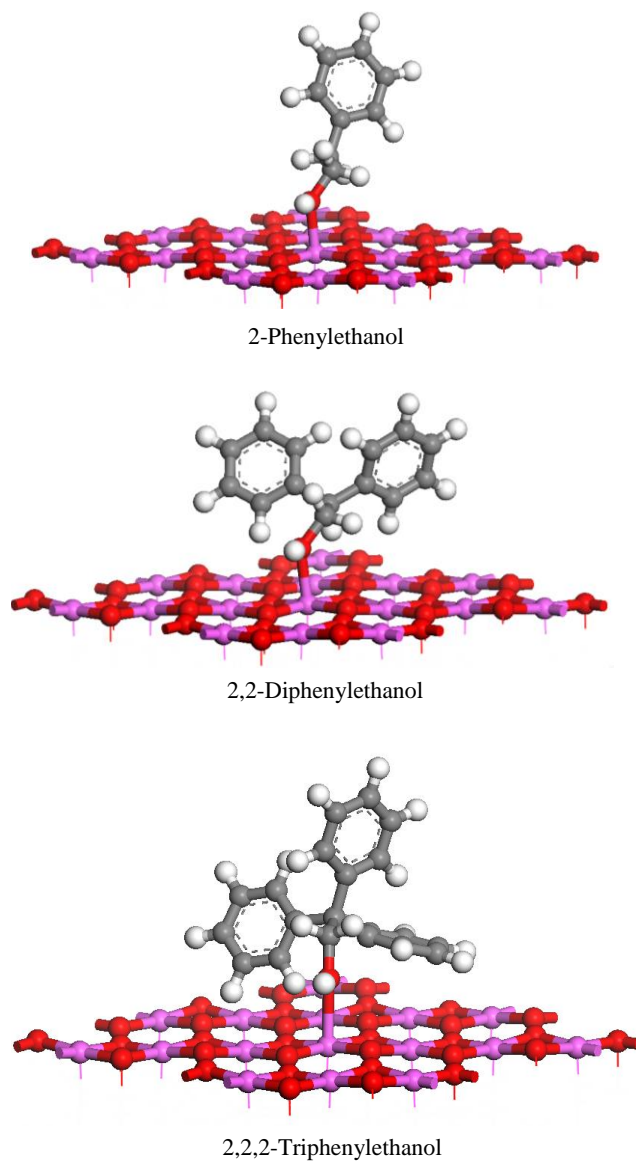


Fig. 2. Continued

3. Results and discussion

The global minimum optimized geometry of considered alcohols after adsorption over nanoscale γ -alumina (1 0 0) surface are shown in Figure 2. Among the primary alkyl substituted alcohols, methanol, ethanol, 1-propanol and 1-butanol are adsorbed over the surface with the adsorption energies of -22.4, -26.0, -26.2 and -27.2 kcal/mol, respectively. Based on these results, the adsorption energy of alkyl alcohols over the surface increases with increasing the alkyl chain length (Table 1). A similar trend is found for secondary alcohols, i.e. -26.2, -27.5 and -38.2 kcal/mol for ΔE_{ads} of 2-propanol, 2-butanol and 2-octanol, respectively.

Ethanol is the smallest alcohol which has both α and β hydrogen atoms. Higher numbers of branch at the α position of ethanol favor the adsorption. For example, the adsorption energy of 2-methyl-2-propanol (*t*-butanol) is -28.6 kcal/mol, which is -2.6 and -2.4 kcal/mol higher (more negative) than ethanol and 2-

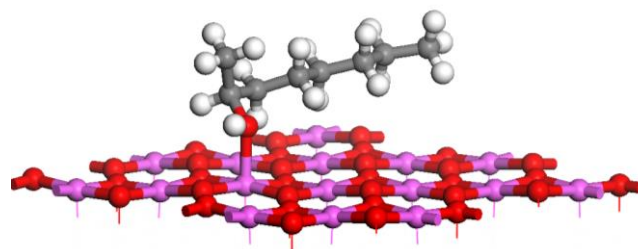
propanol, respectively. Therefore, tertiary alcohols are adsorbed stronger than secondary and primary alcohols over the surface.

The adsorption energies of 2-methyl-1-propanol and 2,2-dimethyl-1-propanol are -25.1 and -23.6 kcal/mol, respectively; which are -1.1 and -2.6 kcal/mol lower (less negative) than ΔE_{ads} of 1-propanol. Therefore, replacements of the β hydrogen atoms of ethanol with the alkyl substituents decrease the adsorption energy. This effect for secondary alcohols is more significant than that for primary alcohols. For instance, the adsorption energies of 3-methyl-2-butanol and 3,3-dimethyl-2-butanol are -25.4 and -23.8 kcal/mol respectively; which are -2.1 and -3.7 kcal/mol lower than the corresponding value for 2-butanol. This decrease in the adsorption energy is associated with increasing the $\text{Al}_{\text{alumina}}-\text{O}_{\text{alcohol}}$ bond distance (Table 1).

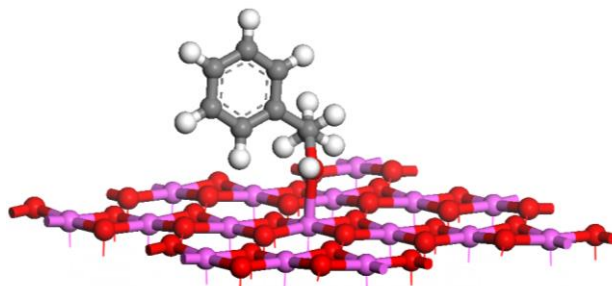
The attraction and repulsion interactions are responsible for the adsorption selectivity of alcohols over the surface. An increase of ΔE_{ads} with increasing the length of alkyl chain or more branches at α position is due to the attractive interactions of alkyl groups by the surface (electronic effects). A decrease of ΔE_{ads} with increase in branching at β position is due to the repulsive interactions of substituents with the surface (steric effects).

Table 1. Adsorption energy and $\text{Al}_{\text{alumina}}-\text{O}_{\text{alcohol}}$ bond distance of alcohols over nanoscale (1 0 0) surface of γ -alumina calculated at BLYP/DNP level of theory

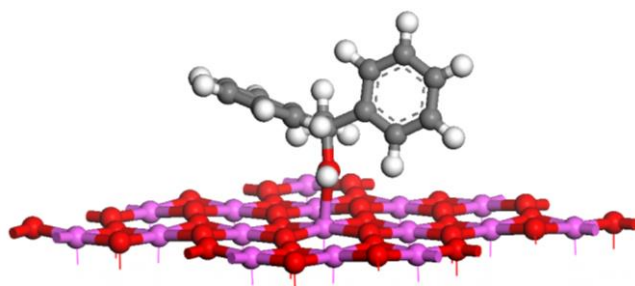
Alcohols	Adsorption energy (kcal/mol)	$\text{Al}_{\text{alumina}}-\text{O}_{\text{alcohol}}$ bond distance (\AA)
<i>Primary alcohols</i>		
Methanol	-22.4	2.056
Ethanol	-26.0	2.040
1-Propanol	-26.2	2.078
1-Butanol	-27.2	2.100
2-Methyl-1-propanol	-25.1	2.086
2,2-Dimethyl-1-propanol	-23.6	2.154
Cyclohexanol	-28.9	2.068
Allyl alcohol	-27.1	2.108
Benzyl alcohol	-28.5	2.206
2-Phenylethanol	-39.2	2.155
2,2-Diphenylethanol	-47.2	2.105
2,2,2-Triphenylethanol	-31.5	2.389
<i>Secondary alcohols</i>		
2-Propanol	-26.2	2.089
2-Butanol	-27.5	2.086
3-Methyl-2-butanol	-25.4	2.138
3,3-Dimethyl-2-butanol	-23.8	2.195
2-Octanol	-38.2	2.051
1-Phenylethanol	-36.4	2.106
<i>Tertiary alcohols</i>		
2-Methyl-2-propanol	-28.6	2.057
Phenol	-31.9	2.054
1,1-Diphenylethanol	-42.7	2.085
1,2-Diphenyl-2-propanol	-49.4	2.082



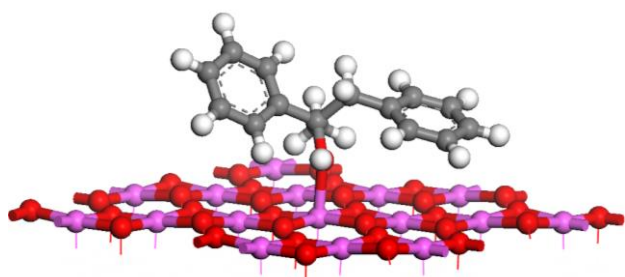
2-Octanol



1-Phenylethanol



1,1-Diphenylethanol



1,2-Diphenyl-2-propanol

Fig. 2. Continued

The aryl groups are adsorbed stronger over the surface than the alkyl and allyl moieties. The adsorption energy of benzyl alcohol is -28.5 kcal/mol, which is -6.1 and -1.4 kcal/mol higher (more negative) than the ΔE_{ads} of methanol and allyl alcohol, respectively. This is due to the larger electronic cloud (charge density) of the phenyl ring (in compare to alkyl or allyl chains) which interacts with the

surface acid sites and provides the greater stabilization (Fig. 3). The adsorption energy of cyclohexanol is slightly higher than benzyl alcohol (-28.9 kcal/mol) which is due to the attractive interaction between axial hydrogen atoms of cyclohexanol and the oxygens of the alumina surface. Also, the conformation of benzyl alcohol after adsorption (the methylene group and phenyl are eclipsed) is less stable than that of before adsorption (the methylene group and phenyl are staggered), which reduces the adsorption energy of this compound.

The adsorption energy of phenol and 1-phenylethanol is -31.9 and -36.4 kcal/mol, respectively. Replacement of a α hydrogen of 1-phenylethanol with phenyl substituent increases the ΔE_{ads} . For example, the adsorption energy of 1,1-diphenylethanol is -42.7 kcal/mol, which is -6.3 kcal/mol higher (more negative) than 1-phenylethanol. Substitution of one phenyl at β position increases the attraction of the phenyl groups (higher ΔE_{ads}), however, when two phenyl groups are added to the β position, the adsorption energy is reduced (an increase in repulsion and steric effects). For example, 2,2-diphenylethanol in comparison to 2-phenylethanol and 2,2,2-triphenylethanol have higher adsorption energy (-47.2 versus -39.2 and -31.5 kcal/mol, respectively). The maximum adsorption energy among considered alcohols is achieved when the phenyl groups are found at both α and β positions, i.e. 1,2-diphenyl-2-propanol with ΔE_{ads} of -49.4 kcal/mol.

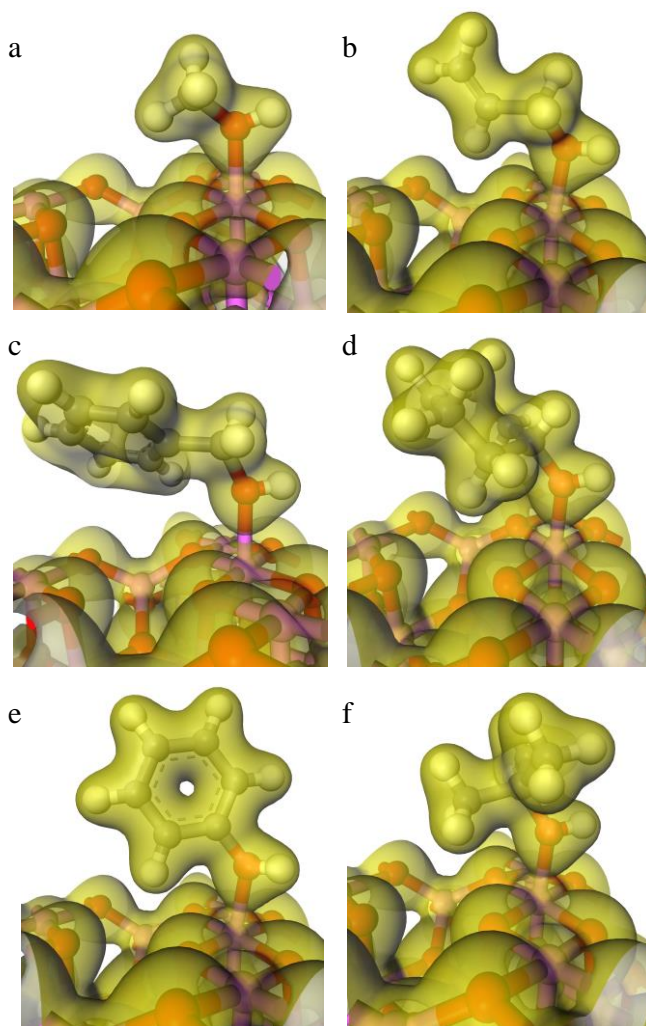


Fig. 3. Total electron density for methanol (a), allyl alcohol (b), benzyl alcohol (c), cyclohexanol (d), phenol (e), and *t*-butanol (f) after adsorption over nanoscale (1 0 0) surface of γ -alumina calculated at BLYP/DNP level of theory

4. Conclusions

In summary, we show that more branches at α position of alcohol increase the adsorption energy, while a decrease in adsorption energy is achieved for alcohols containing the substituents at the β position. The tertiary alcohols are adsorbed over the surface stronger than secondary and primary alcohols. Alcohols with larger alkyl chains have greater adsorption energies. Also the aryl alcohols are adsorbed over the surface better than the alkyl and allyl moieties. The maximum adsorption energy among considered alcohols is obtained where the phenyl groups are found at both α and β positions.

Acknowledgements

We would like to thank the research committee of Malek-ashtar University of Technology (MUT) and Isfahan University of Technology (IUT) for supporting this work. Also, we thank the Computational Nanotechnology Supercomputing Centre, Institute for Research in Fundamental Sciences (IPM), P. O. Box 19395-5531, Tehran, Iran for their kindly supporting in performing some of the computations.

References

1. H. Tachikawa, and T. Tsuchida, *J. Mol. Catal. A Chem.*, 96, 277 (1995).
2. M.B. Fleisher, L.O. Golender, and M.V. Shimanskaya, *J. Chem. Soc. Faraday Trans.*, 87, 745 (1991).
3. H. Kawakami, and S. Yoshida, *J. Chem. Soc. Faraday Trans.*, 81, 1117 (1985).
4. M. Digne, P. Sautet, P. Rayboud, P. Euzen, and H. Toulhoat, *J. Catal.*, 226, 54 (2004).
5. O. Maresca, A. Allouche, J.P. Aycard, M. Rajzmann, S. Clemendot, and F. Hutschka, *J. Mol. Struct. Theochem*, 505, 81 (2000).
6. P. Hirva, and T.A. Pakkanen, *Surf. Sci.*, 277, 389 (1992).
7. M. Lindblad, and T.A. Pakkanen, *Surf. Sci.*, 286, 333 (1993).
8. K.C. Hass, W.F. Schneider, A. Curioni, and W. Andreoni, *Science*, 282, 265 (1998).
9. J. Fernandez Sanz, H. Rabaa, F.M. Poveda, A.M. Marquez, and C. Calzado, *J. Int. J. Quantum Chem.*, 70, 359 (1998).
10. O. Maresca, A. Ionescu, A. Allouche, J.P. Aycard, M. Rajzmann, and F. Hutschka, *J. Mol. Struct. Theochem*, 620, 119 (2003).
11. H.A. Dabbagh, and M. Zamani, *Comput. Mater. Sci.*, 79, 781 (2013).
12. A. Ionescu, A. Allouche, J.P. Aycard, M. Rajzmann, and F. Hutschka, *J. Phys. Chem. B*, 106, 9359 (2002).
13. G. Pacchioni, and N. Rosch, *Surf. Sci.*, 286, 333 (1994).
14. S. Cai, and K. Sohlberg, *J. Mol. Catal. A: Chem.*, 248, 76 (2006).
15. M.L. Ferreira, and E.H. Rueda, *J. Mol. Catal. A: Chem.*, 178, 147 (2002).
16. S. Cai, V. Chihaiia, and K. Sohlberg, *J. Mol. Catal. A: Chem.*, 275, 63 (2007).
17. D.A. De Vito, F. Gilardoni, L. Kiwi-Minsker, P.Y. Morgantini, S. Porchet, A. Renken, and J. Weber, *J. Mol. Struct. Theochem*, 469, 7 (1999).
18. S. Cai, and K. Sohlberg, *J. Mol. Catal. A: Chem.*, 193, 157 (2003).
19. H.A. Dabbagh, M. Zamani, and B.H. Davis, *J. Mol. Catal. A: Chem.*, 333, 54 (2010).
20. H.A. Dabbagh, K. Taban, and M. Zamani, *J. Mol. Catal. A: Chem.*, 326, 55 (2010).
21. G. Feng, C. Huo, C. Deng, L. Huang, Y. Li, J. Wang, and H. Jiao, *J. Mol. Catal. A: Chem.*, 304, 58 (2009).
22. Z. Zuo, W. Huang, P. Han, Z. Gao, Z. Li, *Appl. Catal. A Gen.*, 408, 130 (2011).
23. Z. Zuo, P. Han, J. Hu, W. Huang, *J. Mol. Model.*, 18, 5107 (2012).
24. J.B. Peri, *J. Phys. Chem.*, 69, 220 (1965).
25. H. Knozinger, and C. Ratnasamy, *Catal. Rev. Sci. Eng.*, 17, 31 (1978).
26. G. Busca, V. Lorenzelli, G. Ramis, and R. Willey, *Langmuir*, 9, 1492 (1993).
27. K. Sohlberg, S.J. Pennycook, and S.T. Pantelides, *J. Am. Chem. Soc.*, 121, 7493 (1999).
28. A. Vijay, G. Mills, and H. Metiu, *J. Chem. Phys.*, 117, 4509 (2002).
29. J. Handzlik, J. Ogonowski, and R. Tokarz-Sobieraj, *Catal. Today*, 101, 163 (2005).

30. S. Cai, M. Caldararu, V. Chihai, C. Munteanu, C. Hornoiu, and K. Sohlberg, *J. Phys. Chem. C*, 111, 5506 (2007).
31. M. Digne, P. Sautet, P. Rayboud, P. Euzen, and H. Toulhoat, *J. Catal.*, 211, 1 (2002).
32. M.C. Valero, P. Rayboud, and P. Sautet, *J. Phys. Chem. B*, 110, 1759 (2006).
33. M. Digne, P. Rayboud, P. Sautet, B. Rebours, and H. Toulhoat, *J. Phys. Chem. B*, 110, 20719 (2006).
34. T. Taniike, M. Tada, Y. Morikawa, T. Sasaki, and Y. Iwasawa, *J. Phys. Chem. B*, 110, 4929 (2006).
35. H.P. Pinto, R.M. Nieminen, and S.D. Elliott, *Phys. Rev. B*, 70, 125402 (2004).
36. A. Dyan, P. Cenedese, and P. Dubot, *J. Phys. Chem. B*, 110, 10041 (2006).
37. J. Handzlik, and P. Sautet, *J. Catal.*, 256, 1 (2008).
38. C. Wolverton, and K.C. Hass, *Phys. Rev. B*, 63, 24102 (2000).
39. X. Krokidis, P. Rayboud, A. E. Gobichon, B. Rebours, P. Euzen, and H. Toulhoat, *J. Phys. Chem. B*, 105, 5121 (2001).
40. M. Sun, A.E. Nelson, and J. Adjaye, *J. Phys. Chem. B*, 110, 2310 (2006).
41. A.E. Nelson, M. Sun, and J. Adjaye, *J. Phys. Chem. B*, 110, 20724 (2006).
42. A.R. Ferreira, M.J.F. Martins, E. Konstantinova, R.B. Capaz, W.F. Souza, S.S.X. Chiaro, and A.A. Leitão, *J. Solid State Chem.*, 184, 1105 (2011).
43. H. Knozinger, H. Buhl, and K. Kochloefl, *J. Catal.*, 24, 57 (1972).
44. B.H. Davis, *J. Catal.* 26, 348 (1972).
45. B. Shi, B.H. Davis, *J. Catal.* 157, 359 (1995).
46. B. Delley, *J. Chem. Phys.*, 92, 508 (1990).
47. B. Delley, *J. Chem. Phys.*, 113, 7756 (2000).